Med Chem Res
DOI 10.1007/s00044-016-1653-4

MEDICINAL CHEMISTRY RESEARCH

ORIGINAL RESEARCH

Mononuclear transition metal complexes containing iodo-imidazole ring endowed with potential anti-*Candida* activity

Mohmmad Younus Wani[1] · Aijaz Ahmad[2] · Manzoor Ahmad Malik[3] · Abilio J.F.N. Sobral[1]

Received: 25 April 2015 / Accepted: 4 July 2016

Abstract Special attention is directed to design and synthesize antimicrobial drug candidates by the complexation of bioactive ligands with transition metals. In this pursuit a ligand with imidazole ring was synthesized and treated with Cu^{II}, Co^{II} and ,Ni^{II} salts to afford the mononuclear metallic complexes **IHC1**, **IHC2** and **IHC3,** respectively, being assigned the general formula $[M(L)_2]$. Physical and spectral characterization supported octahedral geometry for the complexes. Both the ligand and the synthesized metal complexes were evaluated for their antifungal activity against three different strains of *Candida*, by determining the minimum inhibitory concentrations and minimum fungicidal concentrations. The antifungal activity results showed that the target compounds display remarkable antifungal activity, with metal complex **IHC1** showing the most potent antifungal activity. Mechanism of action of the ligand and metal complexes appears to originate from membrane disruption as revealed by confocal scanning laser microscopy.

Keywords Hydrazone · Imidazole · *Candida* · Metal complexes · Confocal microscopy

Introduction

In antifungal drug designing, the lack of selectivity of conventional chemotherapeutic agents and the acquisition of multiple-drug resistance are two major challenging problems. With the frequent use of antifungal drugs, resistance has become a global concern (Chi et al., 2011; Kathiravan et al., 2012). The clinical efficacy of many existing antifungal drugs is being threatened by the emergence of multidrug resistant pathogens (Vandeputte et al., 2012). Despite the currently applied antifungal therapies, both mortality and morbidity caused by human pathogens are still unacceptably high (Poulain, 2013). Besides increasing the morbidity and mortality rates, resistance to conventional drugs have resulted in treatment failures and increased health care costs. Therefore, new prophylactic and therapeutic strategies are urgently needed to prevent fungal infection.

Various attempts have been undertaken in this pursuit and an effective drug designing strategy is the complexation of bioactive ligands with transition metal complexes. Among the important pharmacophores responsible for antifungal activity, the azole scaffold is still considered a viable lead structure for the synthesis of more efficacious and broad-spectrum antimicrobial agents. Modifying the structure of the so far effective azole drugs in order to

Electronic supplementary material The online version of this article (doi:10.1007/s00044-016-1653-4) contains supplementary material, which is available to authorized users.

✉ Abilio J.F.N. Sobral
asobral@ci.uc.pt

Manzoor Ahmad Malik
wani@uc.pt

[1] Departmento de Quimica, FCTUC, Universidade de Coimbra, Rua Larga, 3004-535 Coimbra, Portugal

[2] Department of Clinical Microbiology and Infectious Diseases, School of Pathology of NHLS and University of the Witwatersrand, Faculty of Health Sciences, 2193 Johannesburg, South Africa

[3] Department of Chemistry, Jamia Millia Islamia (Central University), New Delhi 110025, India

Published online: 09 August 2016

improve their antimicrobial potency and selectivity is of scientific focus (Liu et al., 2008; Giraud et al., 2008).

Imidazole ring is a part of many existing drugs and the interesting and versatile biological activities of imidazoles established them as important pharmacophores (Sadek, 2011; Zhang et al., 2014). Additionally, acyl-hydrazones exhibit keto-enoltautomerism and –CO–NH–N< moiety of these molecules is suggested to be responsible for their important biological activities (Rollas and Kucukguzel, 2007). A significant number of transition metal complexes of acyl-hydrazones are known for wide spectrum of biological activities, therefore a successful drug development strategy is the complexation of transition metals with such ligands, as it is possible to enhance the pharmacological and chemical properties (such as potency, selectivity, chemical stability and lipophilicity) of the target compounds (Stadler and Harrowfield, 2009; Nandy et al., 2015; Babahan et al., 2015). Another important fact is that the metals can coordinate with O- or N-terminals from proteins in a variety of models and play a crucial role in the conformation and function of biological macromolecules (Bruijnincx and Sadler, 2008).

Considering our previous work on azoles (Wani et al., 2012; Wani et al., 2012; Wani et al., 2013) and taking inspiration from the above facts, in this study we synthesized imidazole ring bearing ligand with a hydrazone pendent and its metal complexes as antifungal leads and made an attempt to unravel the mechanism of action of the synthesized compounds by confocal microscopy.

Materials and methods

Chemistry

Solvents and organic reagents were purchased from Sigma Aldrich and Merck (Germany) and were used without further purification. Melting points (mps) were performed using a Mel-temp instrument, and the results are uncorrected. Elemental analyses were performed on HeraeusVario EL III analyzer. The results were within ±0.4 % of the theoretical values. The absorption spectra were recorded using an OCEAN OPTICS USB 4000 UV spectrometer. IR spectra were recorded on Perkin-Elmer model 1600 FT IR RX1 spectrophotometer as KBr discs or ATR mode. ^{1}H and ^{13}C-NMR spectra were recorded at ambient temperature on a Bruker AVANCE 400 NMR spectrometer using standard parameters. All chemical shifts are reported in δ units with reference to TMS. The FAB mass spectra of all the complexes were recorded on a JEOL SX 102/DA-6000 Mass Spectrometer/Data System using argon/xenon (6 kV, 10 mA) as the FAB gas and m-nitro benzyl alcohol (NBA) as the matrix. Thermogravimetric analysis of the complexes was performed on a TG 51 thermogravimetric analyzer under nitrogen atmosphere with the heating rate of 10 °C min^{-1}. Reactions were monitored using thin-layer chromatography using commercially available precoated plates (Merck Kieselgel 60 F_{254} silica). Visualization was achieved with UV light at 254 nm or I_2 vapour staining.

General procedures for the synthesis of ligand (L)

*Synthesis of ethyl 2-(5-iodo-2-methyl-1H-imidazole-1-yl) acetate (**2**)*

A mixture of 5-iodo-2-methyl-1H-imidazole **(1)** (1 mmol), ethylchloroacetate (1 mmol) and potassium carbonate (1.5 mmol) in dry acetone (5–10 mL) was refluxed for 50 h. The reaction mixture was filtered hot and the solvent was distilled off from the filtrate. The crude ester thus obtained was purified by recrystallization from ethanol.

Yield: 62.5 %; anal. calc. For $C_8H_{11}N_2O_2$: C 32.67, H 3.77, N 9.53 %; found: C 32.48, H 3.92, N 9.23 %; IR ν_{max} cm^{-1}: 3028 (C–H, Ar), 1722 (C=O), 1635 (C=N), 1584 (C=C, Ar), 758 (C–I);^{1}H NMR ($DMSO_d$) δ(ppm): 7.91 (s, 1H, imidazole ring), 4.80 (s, 2H, CH_2), 4.10 (q, 2H, CH_2); 2.20 (s, 3H, CH_3, imidazole ring), 1.35 (t, 3H, CH_3, $J = 6.8$, Hz); ^{13}C-NMR ($DMSO_d$) δ (ppm): 164.21 (C=O) 148.51 (C=N), 128.50, 126.08 (C=C, imidazole ring), 64.51 (–O–CH_2), 48.24 (CH_2), 16.15 (CH_3), 14.11 (CH_3, imidazole ring); FAB MS m/z: 294.06 $[M + H]^+$, 317.18 $[M + Na]^+$.

*Synthesis of 2-(5-iodo-2-methyl-1H-imidazol-1-yl) acetohydrazide (**3**)*

2-(5-iodo-2-methyl-1H-imidazol-1-yl)acetohydrazide (**3**) was synthesized as by a reported procedure (Wani et al., 2013).

Yield 70 %; anal. calc. for $C_6H_9N_4O$: C 25.73, H 3.24, N 20.00 %; found: C 25.45, H 3.42, N 20.26 %;IR ν_{max} cm^{-1}: 3280 (NH), 3022 (C–H, Ar), 1711 (C=O), 1628 (C=N), 1595 (C=C, Ar), 786 (C–I);^{1}H NMR ($DMSO_d$) δ (ppm): 8.32 (bs, 1H, NH), 7.68 (s, 1H, imidazole ring), 4.74 (s, 2H, CH_2), 2.34 (s, 3H, CH_3) 2.18 (d, 2H, NH_2); ^{13}C-NMR ($DMSO_d$) δ (ppm): 162.11 (C=O) 148.48 (C=N), 128.30, 126.10 (C=C, imidazole ring), 26.15 (CH_2), 12.15 (CH_3, imidazole ring); FAB MS m/z: 281.05 $[M + H]^+$.

Synthesis of the ligand

*(2-(5-iodo-2-methyl-1H-imidazol-1-yl)-N′-((pyridin-2-yl) methylene)acetohydrazide) **L***

2-Pyridinecarbaldehyde (10 mmol) was added over a solution consisting of 2-(5-iodo-2-methyl-1H-imidazol-1-yl)

acetohydrazide (**3**) (10 mmol) in 20 ml ethanol and the reaction mixture was kept under reflux for about 3 h. The solvent was removed under reduced pressure and the microcrystalline mass obtained was recrystallized from methanol.

Yield: 89.5 %; IR $\nu_{max}cm^{-1}$: 3570 (NH), 3022 (C–H, Ar), 1675 (C=O), 1628 (C=N), 1595 (C=C, Ar);^{1}H NMR ($DMSO_d$) δ (ppm): 8.69 (bs, 1H, NH), 8.38–7.54 (m, 4H, Ar), 7.38 (s, 1H, imidazole ring), 7.30 (s, 1H, CH), 4.72 (s, 2H, CH_2), 2.36 (s, 3H, CH_3); ^{13}C-NMR ($DMSO_d$) δ (ppm): 168.12 (C=O) 152.64 (C=N, pyridine ring), 148.48 (C=N, imidazole ring), 148.11 (C=C, pyridine ring), 138.63 (C=N, hydrazone),136.12, 129.10 (C=C, pyridine ring), 128.30, 126.10 (C=C, imidazole ring), 26.45 (CH_2), 12.28 (CH_3, imidazole ring); FAB MS m/z: 369.03 $[M^+ + H]^+$, 392.08 $[M^+ + Na]^+$.

Synthesis of the metal complexes

To a hot solution of the ligand (**L**), (2 mmol) in methanol (10 mL) was added a solution of respective metal chloride salt (Cu, Co, Ni) (1 mmol) dissolved in minimum quantity of ethanol and the reaction mixture was heated under reflux for 3–4 h. After keeping the solution at 0 °C overnight, the coloured solid separated out. This was filtered off and washed with hot water followed by small quantity of ethanol and dried to give amorphous solids in 65–75 % isolated yield. (For spectral data see supporting information).

Biology

Strains and media

Stock cultures of the *C. albicans*, *C. glabrata* and *C. tropicalis* were maintained on nutrient agar slants and stored at 4 °C. Prior to experiment, cells were grown and sub-cultured in yeast extract, peptone and dextrose (YPD) media at 37 °C in orbital shaker at 200×rpm (REMI CIS 24 BL). Prior to each experiment, overnight grown microorganism suspensions in YPD broth were standardized to 10^6 CFU/mL.

Determination of minimum inhibitory concentrations (MIC) and minimum fungicidal concentrations (MFC)

Minimum inhibitory concentration was defined as the lowest concentration of the test compound that causes inhibition of visible growth (turbidity). MIC was determined in vitro in liquid medium by the macrobroth dilution method as per the guidelines of CLSI reference document M27-A3 (CLSI, 2008). Positive control fluconazole, negative vehicle control (1 % DMSO) and culture control were also included in every set of experiments. To determine MFC values, after reading the corresponding MIC values, 20 µL samples from all optically clear tubes (complete growth inhibition) plus the last tube showing growth were sub-cultured on YPD agar plates. The plates were incubated at 37 °C for a minimum of 3 days, until growth was clearly visible in the control samples, and MFC values were determined as the lowest concentration of the test compounds for which there was no visible growth on plates.

Disc diffusion halo assays

Strains were inoculated into liquid YPD medium and grown overnight at 37 °C. The cells were then pelleted and washed three times with distilled water. Approximately, 10^5 cells/mL were inoculated in molten agar media at 40 °C and poured into 100 mm diameter petriplates. Filter discs were kept on solid agar and test compounds were spotted on the disc. Test compounds (four fold more than MIC) were pipetted onto 4 mm diameter filter discs and the plates were incubated for 48 hours at 37 °C. After incubation period, the diameter of zone of inhibition was recorded in millimetres and was compared with that of control. Experiments were performed thrice in replicate on separate days and values were calculated in terms of meanof all three respective categories.

Growth curve studies

To further check the effect of the ligand and its metal complexes on the growth of the *Candida* cells, growth curve study was performed as described previously (Khan et al., 2010). *Candida* cells from the overnight grown primary culture were inoculated into 100 mL of fresh YPD broth and incubated at 37 °C for 24 h. Both ligand and its metal complexes were added at MIC and half MIC values to the cultures along with the positive and negative controls. After every 2 h aliquots were taken and growth was recorded turbidometrically at 595 nm using a LaboMed Inc. Spectrophotometer (USA). All the experiments were done in triplicate and the results were shown as mean ± standard deviation.

Confocal scanning laser microscopy (CSLM)

Confocal scanning laser microscopy (CSLM) was used to evaluate the effect of test compounds on the architecture of yeast cells using propidium iodide (PI). PI is a fluorescent probe used to study the effect of drugs on membranes. It only penetrates cells with severe membrane lesions, showing increased red fluorescence (Ahmad et al., 2011; Naskar et al., 2005). *Candida albicans*cells (10^6/mL) were incubated at 37 °C up to mid-exponential phase and were then

treated with four times MIC of test compounds along with negative (no compound) and positive (5 mg/L amphotericin B) controls. The samples were then inoculated at 37 °C for 30 min, in dark. Unstained cells were always included as auto-fluorescence controls. The suspensions were centrifuged, washed and resuspended in phosphate-buffered saline. Five microlitres of PI were added to the cell suspensions in order to obtain a final concentration of 1 mg/L to determine the changes in cellular morphology. The cells were examined with Olympus Laser Confocal Scanning Microscope equipped with green helium neon laser (543 nm) for PI. The objective used was an oil immersion C-Apochromat lens (20×). Image acquisition was done by FV10-ASW1.6 Software.Four different slots per slide were selected independently and stained and unstained cells were counted. All the experiments were done in triplicate and percentage of stained dead cells were shown as mean of these counts.

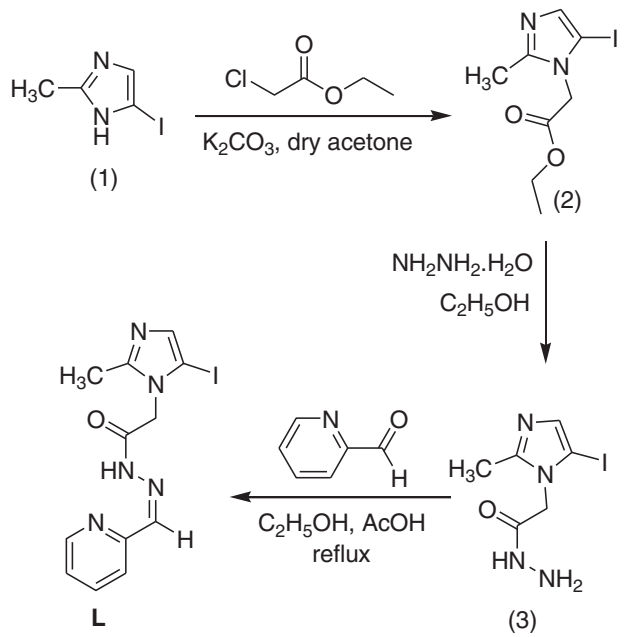

Scheme 1 Synthesis of ligand (**L**)

Results and discussion

Chemistry

The starting material 5-iodo-2-methyl-1H-imidazole **(1)** employed in the preparation of the ligand was obtained from Sigma and used after purification by recrystallization. 2-(5-iodo-2-methyl-1H-imidazol-1-yl)acetohydrazide (**3**) was obtained by refluxing the starting material **1** with ethylchloroacetate under basic conditions and subsequent treatment with hydrazine hydrate in ethanol**.** Final step involved the treatment of acetohydrazide (**3**) with equimolar ratio of 2-pyridine carboxaldehyde in ethanol (Scheme 1). The ligand (**L**) was obtained in 75 % yield and recrystallized from ethanol and found to be highly soluble in methanol, ethanol, DMSO, DMF, acetonitrile, dichloromathane and chloroform. Structure was established by FTIR, ^{1}H NMR, ^{13}C-NMR and FAB MS spectral analysis.

The complexes were prepared by mixing 2:1 ratio of the appropriate ligand (**L**) and metal chloride salts (Cu, Co, Ni) in ethanol under reflux for 3–4 h (Scheme 2). After keeping the solution at 0 °C overnight the coloured solid separated out. This was filtered off and washed with hot water followed by small quantity of methanol, and dried in *vacuo* over silica gel to give amorphous solids with >75 % yield. Our attempt to get single crystals of the complexes was a failure. The obtained complexes are stable in air, are soluble in DMF, DMSO, sparingly soluble in MeOH, EtOH and DCM, but insoluble in water and having mps higher than 300 °C. The molar conductance values in DMSO (10^{-3} M) are too low to account for any dissociation, therefore the complexes are considered to be non-electrolytes (Chandra et al., 2009). **IHC1**, **IHC2** and **IHC3** showed value of 28, 36 and 29 Ω^{-1} cm^2 mol^{-1}, respectively. The elemental

Scheme 2 Synthesis of metal complexes (**IHC1**–**IHC3**)

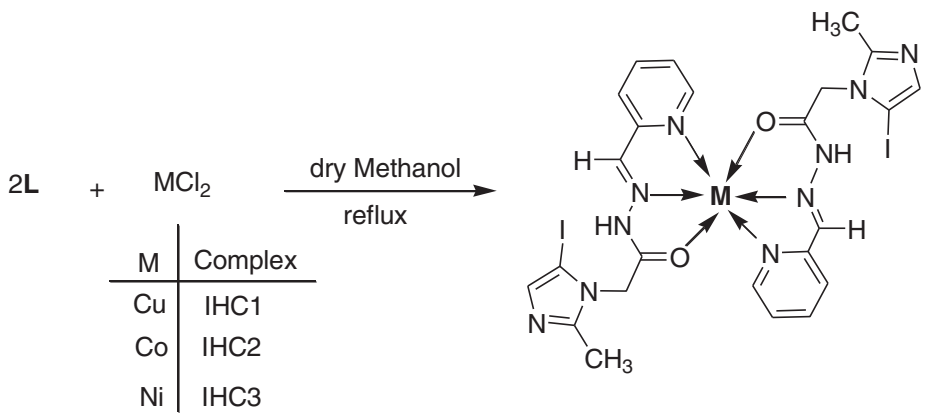

analyses data along with some physical properties of the ligand (**L**) and its complexes (**IHC1**, **IHC2** and **IHC3**) are reported in Table 1. The chemical structures of all the compounds were confirmed by means of elemental analysis and electronic, IR, ^{1}H NMR and ^{13}C-NMR spectral studies. The structures of complexes were further established by thermogravimetric analysis and FAB MS. The analytical data of these compounds are in good agreement with their composition.

Selected significant IR bands revealed the structural characteristics of the compounds. The Ligand (**L**) may exhibit keto-enol tautomerism since it contains a keto group (C=O) and a proton adjacent to carbonyl group (Fig. 1). The absence of υ (OH) stretch at 3550–3200 cm^{-1} and the presence of υ (N–H) stretch at 3570 cm^{-1} in the spectra of the ligand suggest that the ligand remains in the keto form in the solid state. The amide C=O stretch at 1675 cm^{-1} of ligand is shifted to lower wave number by ca. 15–30 cm^{-1}, indicating that it participates as a coordinating site. This coordination behaviour of the ligand is also proved by the appearance of IR bands due to υ M–O and υ M–N vibrations in the range 478–498 cm^{-1} and 428–450 cm^{-1}, respectively (Abu-Melha and El-Metwally, 2007; Chandra and Sharma, 2009). The pyridine-ring-stretching, in-plane-ring-bending and out of-plane-ring-bending vibrations are found at 1502, 628 and 502 cm^{-1}, respectively. These absorptions are highly affected when nitrogen atom of pyridine ring takes part in coordination. The position of these absorption bands is shifted to higher region, indicating that the nitrogen of pyridine ring is involved in coordination. The negative shift of 25–50 cm^{-1}of υ (C=N) stretch in the complexes indicates the involvement of azomethine nitrogen in complexation (Lever, 1968). The broad band observed in region 3570 cm^{-1} due to υ (N–H) stretch is slightly shifted in complex probably due to the adjustment of current arising due to coordination of amide C=O, thus, confirming the fact that ligand behaves as a neutral tridentate NNO donor in these complexes.

The UV-vis spectroscopy is a versatile technique, which enables establishing structure of metal complexes with utmost certainty. Electronic spectra of the ligand, shows two bands at 255 nm and 335 nm due to the benzene ring and the $\pi\rightarrow\pi^*$ transition of the chromophores (–C=N–NH–CO–), respectively. These bands get red shifted by 5–10 nm and 10–40 nm respectively, in the electronic spectra of the complexes. In addition to ligand-originated bands, additional absorption bands due to metal-originated d-d transitions and charge transfer spectra were observed in the spectra of the complexes, characteristic to their geometries. The electronic spectra of the copper (II) complex (**IHC1**) display bands at 770 nm and 368 assigned to $^{2}B_{1g}\rightarrow{}^{2}E_{g}$ transitions and, charge transfer bands (L→Cu^{II} CT), respectively, indicating its tetragonally distorted octahedral geometry (Yan-Hui et al., 2007; Lever, 1968). This complex has magnetic moment 1.96 BM, which is higher than the spin-only value (1.70 BM) expected for one unpaired electron and offers possibility of an octahedral geometry (Singh et al., 2007). Cu^{II} ion has one unpaired electron in the 3d shell, therefore, its compounds have magnetic moment close to spin-only value of 1.73 BM. Due to spin orbital coupling, higher values are observed. Cobalt(II) complex (**IHC2**) gave rise to three absorption bands in the

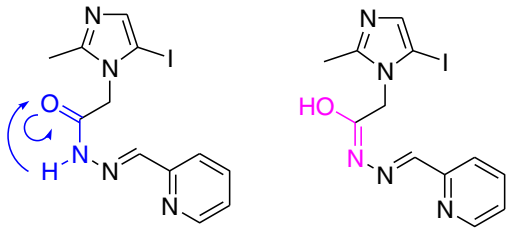

Fig. 1 Possible Keto-Enol tautomerism of the Ligand (**L**) (A = Keto; B = Enol)

Table 1 Elemental analyses data along with some physical properties of the ligand (**L**) and its complexes (**IHC1**, **IHC2** and **IHC3**)

Compound	Molecular formula	MW calculated	Elemental analysis				$\Lambda\ \Omega^{-1}$ cm^{2}mol^{-1}	μ (BM)
			C	H	N	M		
L	$C_{12}H_{12}N_5OI$	369.03	39.04	3.28	18.97	—	—	—
			39.28	3.40	18.78			
IHC1	$(C_{24}H_{24}N_{10}O_2I_2Cu)$	802.84	35.95	3.02	17.47	7.48	28	1.96
			36.15	3.12	17.22	7.60		
IHC2	$(C_{24}H_{24}N_{10}O_2I_2Co)$	797.92	36.15	3.03	17.57	10.98	36	4.85
			36.35	3.18	17.76	10.72		
IHC3	$(C_{24}H_{24}N_{10}O_2I_2Ni)$	797.95	36.17	3.04	17.57	7.36	29	2.75
			56.10	3.22	17.85	7.58		

MW Molecular Weight, *Molar conductance* $\Lambda\ \Omega^{-1}$ cm^{2}mol^{-1}, *Magnetic moment* μ (BM)

visible region, under the influence of octahedral field, by the excitation of the electron from the ground state $^4T_{1g}(F)$ to the excited states $^4T_{2g}(F)$, $^4A_{2g}(F)$ and $^4T_{1g}(P)$. 940 nm assigned to $^4T_{1g}(F) \rightarrow {}^4T_{2g}(F)$ ν_1, 710 nm assigned to $^4T_{1g}(F) \rightarrow {}^4A_{2g}(F)$ ν_2, and 440 nm assigned to $^4T_{1g}(F) \rightarrow {}^4T_{1g}(P)$ ν_3 transitions in a high-spin d^7 octahedral environment (Rakha et al., 2014). The room temperature magnetic moment value of 4.85 BM demonstrates that **IHC2** is paramagnetic and has a high-spin octahedral configuration with $^4T_{1g}(F)$ ground state (Subramanya et al., 2003). The electronic spectra of Nickel (II) complex (**IHC3**) display three absorption bands at 915, 660 and 395 nm, assigned to $^3A_{2g}(F) \rightarrow {}^3T_{2g}(F)$ υ_1, $^3A_{2g}(F) \rightarrow {}^3T_{1g}(F)$ υ_2 and $^3A_{2g}(F) \rightarrow {}^3T_{1g}(P)$ υ_3, respectively (Ibrahim et al., 2014). The magnetic moment of the Ni(II)complex at room temperature lies in the range of 2.75 BM corresponding to two unpaired electrons. Thus, on the basis of spectral studies complexes **IHC1**, **IHC2** and **IHC3** were assigned to have a six coordinated distorted octahedral geometry as shown in Scheme 2.

Further evidence for the formation of compounds was obtained from the ^1H NMR spectra. Assignments of the signals are based on the chemical shifts and intensity patterns. The ligand (**L**) did not show any resonance at ca. 0.5–5.0 ppm, attributed to –OH proton resonance, while the appearance of a broad peak at 8.63 ppm due to the –NH proton of amide group indicates that even in a polar solvent such as DMSO they remain in the keto form. The –NH proton signal of the ligand usually shifts 1.50–2.50 ppm upfield in the complexes (**IHC1**, **IHC2** and **IHC3**). However, in complexes, we could not calculate the coupling constant values for aromatic region, possibly due to the merging of peaks upon coordination. This information suggests the adjustment of electronic current upon coordination of >C=O group to the metal ion. The aromatic ring protons were observed with the expected chemical shift and integral values in the same region as those of free ligand. Moreover, the ^{13}C-NMR spectra of the ligand taken in DMSO gave the spectral signals in good agreement with the probable structures. The ligand showed two signals at 173.5 and 164.5 ppm assigned to the amide (C=O) and azomethine carbon (C=N), respectively. The signals from 126.8 to 148.5 ppm were due to the imidazole, pyridine and phenyl ring carbons. ^{13}C-NMR spectra were also used for the elucidation of the coordination mode of the ligand in complexes. Assignments of the signals are based on the chemical shifts and intensity patterns and coordination induced shift (CIS), $\Delta\delta$ [$\Delta\delta = \delta$ (complex)$-\delta$ (free ligand)], of the signals for carbon atom in the vicinity of the coordinating functions. Thus the C=O carbon in the ligand experiences CIS value of 5–8 ppm in complexes, indicating the coordination of carbonyl oxygen. As a result of variation of electron density on coordination, azomethine carbon signal is shifted downfield by 2–5 ppm in their respective complexes, which indicates coordination of nitrogen lone pair to metal.

Thermal behaviour of the complexes (**IHC1**, **IHC2** and **IHC3**) was studied in the temperature range 25–900 °C. All the dehydrated complexes are stable upto ca.150 °C and then decompose in three major steps. The temperature range for the first endothermic step being 150–290 °C followed by second exothermic step in the temperature range of 290–380 °C. Differential Thermal Analysis plots for complexes suggest their exothermic nature of decomposition in the subsequent stages. Third stage of decomposition starts immediately after second one and continues until complete decomposition of the ligand and formation of MO (M=Cu, Co, Ni) as the end product. The final temperature at which MO obtained varied from complex to complex, but in any case the formation of final stable product does not go beyond 900 °C. Although decomposed fragments of the ligand could not be approximated due to continuous weight loss, the total percentage of weight loss of the complexes corresponds to the loss of the ligand after considering the transfer of one oxygen atom to the metal ion and residue corresponds to the metal oxide. Additionally, a general splitting pathway with the characteristic peaks was observed by the metal complexes. The positive ion FAB mass spectrum of the complexes was recorded using n-NBA as the matrix. The spectra of the complexes (**IHC1**, **IHC2** and **IHC3**) showed a number of informative fragment ions of different intensities confirming their molecular weights. The mass spectrum of the metal complexes (**IHC1**, **IHC2** and **IHC3**) obeyed a similar pattern of fragmentation with the molecular ion peaks observed as $[M + Na^+ + H]^+$, $[M + K^+ + H]^+$, $[M + Na^+]$ (Metal adduct ions) and $[M + H]^+$ and the major fragmentation pathway involved the cleavage of amide group.

Antifungal Studies

MICs and MFCs

MICs and MFCs of the ligand and its metal complexes have been determined against three different laboratory *Candida* species. Table 2 summarizes the in vitro susceptibilities MICs and MFCs of all the test compounds against these fungal isolates. Evaluation of MIC and MFC values showed that both the ligand and its metal complexes were active in vitro against all the tested isolates, however, the MIC/MFC values of the ligand against all the three types of *Candida* strains were higher when compared to the metal complexes (Table 2, Fig S1), but are within the reference range. The lowest MIC/MFC results obtained with metal complex **IHC1** suggest an increase in the antimicrobial activity after

Table 2 Minimum inhibitory concentrations of **L**, **IHC1**, **IHC2** and **IHC3**

Compound	Mean MIC/MFC (mg/L)		
	C. albicans ATCC 10261	*C. glabrata* ATCC 90030	*C. tropicalis* ATCC 750
L	50/100	50/100	50/100
IHC1	6. 25/12.5	6. 25/12. 5	6. 25/12. 5
IHC2	12.5/25	6. 25/25	6. 25/12.5
IHC3	12.5/100	25/200	25/200
Fluconazole	2	4	8
Amphotericin B	0.125	2	2

the interaction of the ligand with Cu^{II} ions. These results are in congruent with the previous findings where metal complexes were observed to easily disrupt the cell walls leading to cell death (Goulart, 2011; Antonio et al., 2014).

Disc diffusion assay

Index of sensitivity (SI) was defined as the diameter of inhibition zone(mm)/concentration (mg/mL) = clearing (mm/mg). The sequence of the SI for all the test compounds decreases in the order given as **IHC1>IHC2>IHC3>L**. The SI values for **IHC1**, **IHC2**, **IHC3** and **L** are 3.4, 3.2, 2.5 and 1.2, respectively. While variability may occur among the antifungal activity of the test compounds, it is exciting that the complexes except **IHC3** showed fungicidal potential, as is evident from the clear zones of inhibition in disc diffusion assay; whereas in contrast **IHC3** showed a visible turbid halo, an indication of its fungistatic nature (Fig. 2). There was a complete growth observed around the control disc impregnated with the solvent (1 % DMSO), which indicates that all the inhibition of the *Candida* growth is because of the test compounds and not of the solvent.

Growth curve studies

Effect of different concentrations of the ligand and its metal complexes on the growth pattern of *C. albicans*, *C. tropicalis* and *C. glabrata* are shown in Fig. 3 (a–c), respectively. The control *Candida* cells showed a normal pattern of growth, with a lag phase of 2–4 h and an active exponential phase of 14–16 h before attaining the stationary phase. The test compounds suppressed growth and delayed exponential phases of all three tested isolates of *Candida* as shown in Fig. 3. Both the ligand and the complexes affect the growth pattern of *Candida* species almost in a similar manner. At MIC values of the test compounds flat lines were observed indicating the complete inhibition of growth, whereas, ½ MIC values showed reduced growth pattern in comparison with the control. The growth pattern clearly

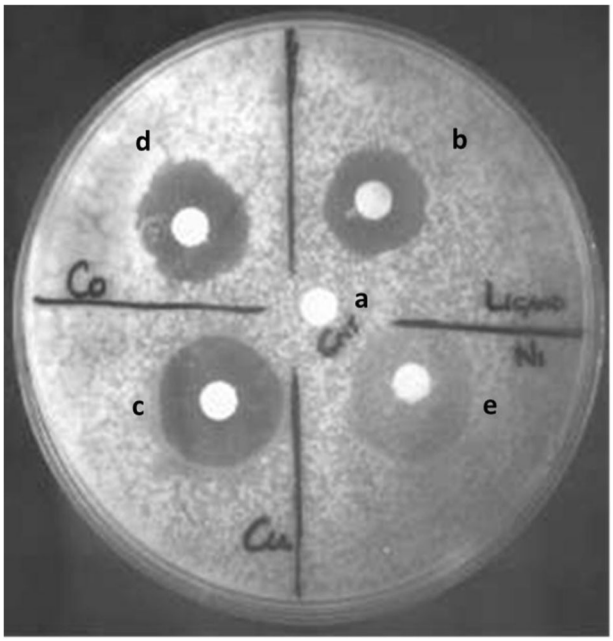

Fig. 2 Representative plate of disc diffusion assay of *C. albicans* 10261 treated with ligand (b), IHC1 (c), IHC2 (d) and IHC3 (e). Negative solvent control (1 % DMSO) is represented by (a) in the centre. Zone of inhibitions were observed after plates were incubated for 48 h at 37 °C

depicts the higher effect of the complexes than the ligand. A known drug (2 mg/Lamphotericin B) was included as a positive control, depicting flat lines with complete inhibition of growth in all the three isolates. Flat lines at MIC values of the ligand and its metal complexes as well as that of known drug against all the three types of *Candida* isolates showed potent antifungal efficacy of the legend and its metal complexes. These results also highlight that the antifungal effects of ligand and its metal complexes are primarily concentration dependent.

Confocal laser microscopy

Candida albicans cells were grown and then stained with PI as described in experimental section. PI penetrates only those cells which have severe membrane lesions; the entire yeast cell appears red. The laser confocal images of stained *Candida* cells exposed to test compounds are shown in Fig. 4. The dead stained cells were counted from four different slots per slide in three different experiments and mean percentage was expressed. Our results showed that maximum of PI penetrates (dead cells) 75 % of the yeast cells when treated with 4×MIC of **IHC1**, while as 65 % cells showed PI uptake when treated with 4×MIC of **IHC2** and 65 % with 4×MIC of **IHC3**. 30 % cells showed PI uptake when treated with 4×MIC of the ligand (**L**). This indicates that the structure of the cell membrane was

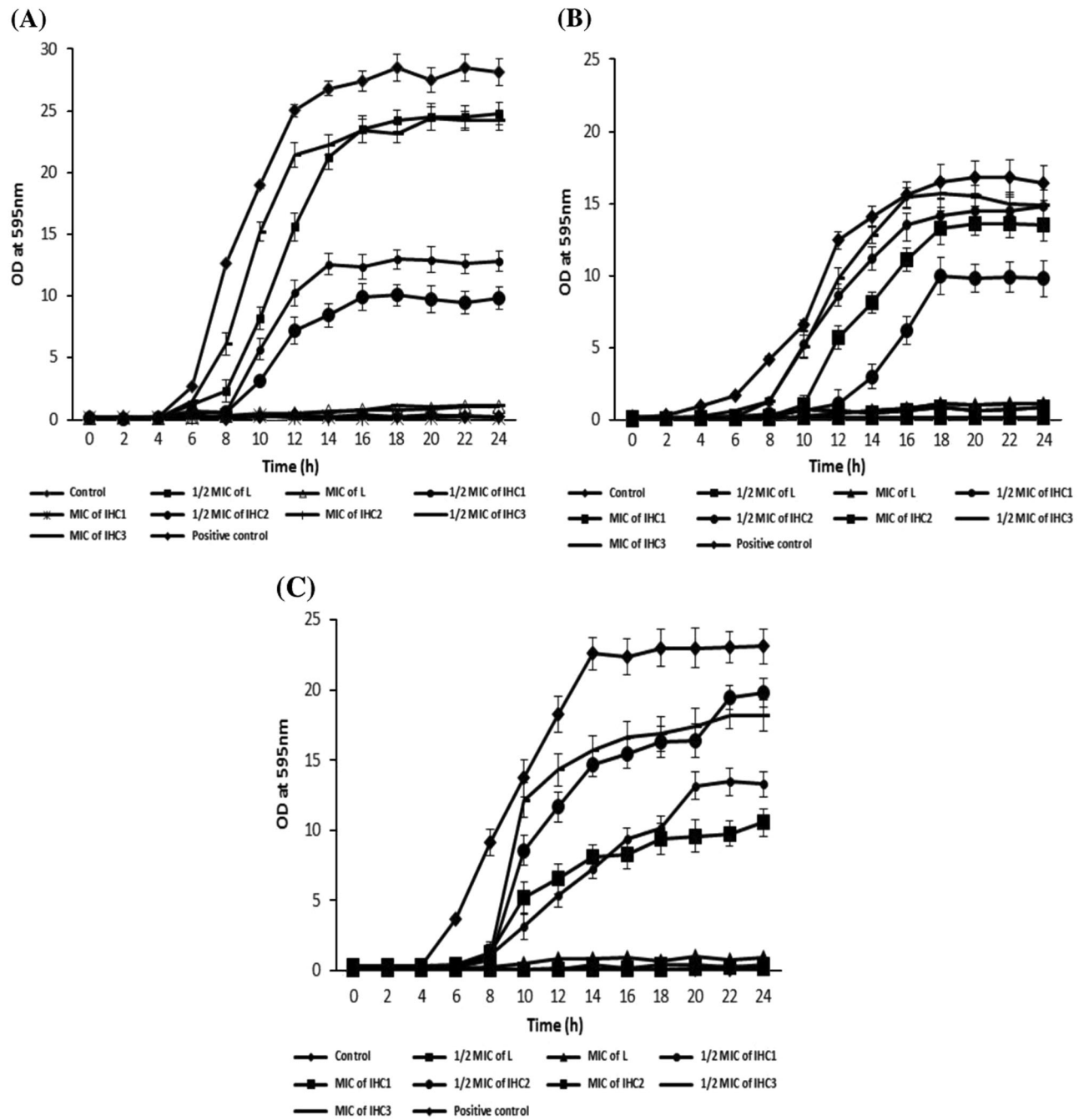

Fig. 3 Growth curve study of representative standard—*Candida albicans* (**a**), *Candida tropicalis* (**b**) and *Candida glabrata* (**c**) isolates grown with half MIC of ligand (*triangles*) and MIC of ligand (plus), half MIC of IHC1 (cyrillic) and MIC of IHC1 (minus), half MIC of IHC2 (stars) and MIC of IHC2 (hyphen), half MIC of IHC3 (circles), and MIC of IHC3 (*black lozenge*). *Squares* and *diamonds* represent negative and positive controls, respectively. Values shown in figure are mean ± SD of three independent recordings

disrupted by these test compounds to a large extent indicating that these compounds display a membrane disruption mechanism of action. Under these conditions, 5 mg/L amphotericin B-induced PI staining in more than 90 % of *Candida* cells (Fig. 4).

This study supports the fact that the lipophilicity of the drug is increased through the formation of chelates with metals and drug action is increased due to effective permeability of the drug into the site of action. In fact, metal complex provide better opportunities to be used as therapeutic agents. The enhanced antifungal activity of the complexes over the ligand can also be attributed to the fact that the acyl-hydrazone ligand contains a polar head; the hydrazide part and an aromatic hydrophobic part. The

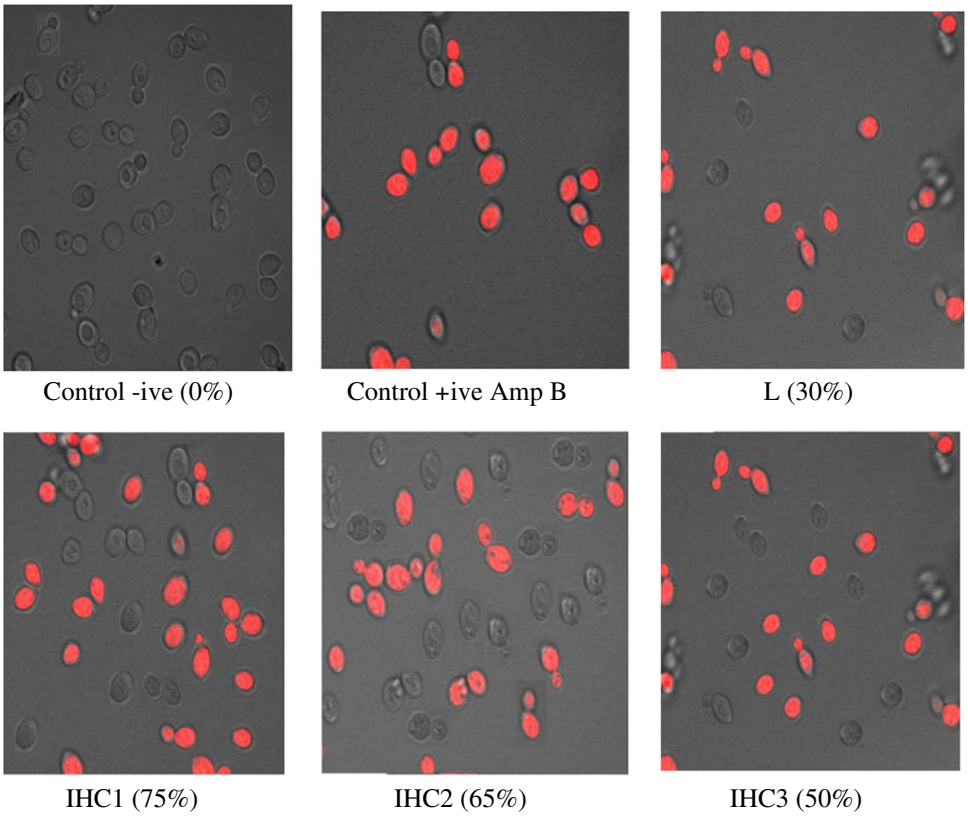

Fig. 4 Laser confocal images of *Candida albicans* cells. Cells with membrane damage are seen stained with PI (*red* signals)

coordination allows the ligand to hide the acyl-hydrazone polar part around the metal and the metal complex thus exposes the hydrophobic moiety to the solvent endowing it of the features necessary to cross the cell membrane. Another assumption is that the combination of two ligands with a divalent metal ion results in a charge neutral complex (Bernhardt et al., 2009). This charge neutrality means that the complexes themselves may also be able to cross the cell membrane, and this provides a novel method of delivery of the compounds to the cell in the form of a labile divalent complex which may then dissociate within the cell (Bernhardt et al., 2009). The reason for high antifungal activity of copper complex (**IHC1**) can be explained in terms of the effect of copper metal ion on the normal cell process. The complexation reaction reduces the polarity of the metal ion by the partial sharing of metal ion positive charge with donor groups and electron delocalization over the chelate ring (Özer et al., 2009). Thus, the lipophilic character of the central metal atom is enhanced that results in a higher capability to penetrate the microorganisms through the lipid layer of the cell membrane.

Rapidity of action and low MIC values of these novel complexes offered an opportunity to develop new antifungals in the continued quest to control important infectious pathogens. However, the need for the second step testing, which involves the trialling of these compounds for toxicity and side effects at cellular levels is highly required. Additional in vitro and in vivo tests are required to be performed on new fungal strains including the resistant species and other pathogens to evaluate antimicrobial potentials of these novel complexes.

Conclusions

In the present paper, we discussed the synthesis of Cu^{II}, Co^{II} *and* Ni^{II} metal complexes of a ligand bearing an iodo-imidazole ring and hydrazone pendent with a pyridine ring. In all complexes, the ligand L acted as a tridentate NNO donor favouring an octahedral geometry. Further antifungal activity evaluation by determining MIC and MFC, disc diffusion assay and growth curve studies revealed that the metal complexes show enhanced activity compared to the ligand that can be attributed to their increased lipophilicity compared to the ligand alone. Laser confocal images showed remarkable membrane disruption due to the target compounds. Therefore, these preliminary results indicate that iodo-imidazole and pyridine ring bearing transition metal complexes can be promising therapeutic agents against fungal infections, which, however, needs further optimization.

Acknowledgments MAM is thankful to UGC India for financial support. Fundação para a Ciência e a Tecnologia (FCT-Portugal) grant SFRH/BPD/86581/2012 (M.Y. Wani) is highly acknowledged.

Compliance with ethical standards

Conflict of interest The authors declare that they have no competing interests.

References

Abu-Melha KS, El-Metwally NM (2007) Synthesis and spectral characterization of some investigated thiocarbohydrazone binuclear complexes with an illustrated EPR study for d^1 complexes. Trans Met Chem 32:828–834

Ahmad A, Khan A, Akhtar F, Yousuf S, Xess I, Khan LA, Manzoor N (2011) Fungicidal activity of thymol and carvacrol by disrupting ergosterol biosynthesis and membrane integrity against *Candida*. Eur J ClinMicrobiol Infect Dis 30:41–50

Antonio FS, Débora FB, Lis RVF, Natália AC, Geziel RA, Margareth B, Alberto AC, Ademir N, Daniela CMR, Ademir dos A (2014) Study of the antimicrobial activity of metal complexes and their ligands through bioassays applied to plant extracts. Rev Brasil Farmacogn 24:309–315

Babahan I, Emirdag-Öztürk S, Poyrazoglu-Çoban E (2015) Spectroscopic and biological studies of new mononuclear metal complexes of a bidentate NN and NO hydrazone–oxime ligand derived from egonol. Spectrochim Acta Part A: Mol Biomol Spectrosc 141:300–306

Bernhardt PV, Sharpe PC, Islam M, Lovejoy DB, Kalinowski DS, Richardson DR (2009) Iron chelators of the dipyridyl-ketone thiosemicarbazone class: precomplexation and transmetalation effects on anticancer activity. J Med Chem 52:407–415

Bruijnincx PC, Sadler PJ (2008) New trends for metal complexes with anticancer activity. Curr Opin Chem Bio 112:197–206

Chandra S, Jain D, Sharma AK (2009) EPR, mass, electronic, IR spectroscopic and thermal studies of bimetallic copper(II) complexes with tetradentate ligand, 1,4-diformyl piperazinebis (carbohydrazone). Spectrochim Acta A MolBiomolSpectrosc 71:1712–1719

Chandra S, Sharma AK (2009) Nickel(II) and copper(II) complexes with Schiff base ligand 2,6-diacetylpyridine bis(carbohydrazone): synthesis and IR, mass, (1)H NMR, electronic and EPR spectral studies. Spectrochim Acta A MolBiomolSpectrosc 72:851–857

Chi HW, Yang YS, Shang ST, Chen KH, Yeh KM, Chang FY, Lin JC (2011) *Candida albicans* versus non-albicans bloodstream infections: the comparison of risk factors and outcome. J Microbiol Immunol Inf 44:369–375

CLSI (Clinical and Laboratory Standard Institute), (2008) Approved Standard M27-A3, Clinical and Laboratory Standard Institute, Fort Wayne, Ind, USA, 25 pp.

Giraud F, Loge C, Pagniez F, Crepin D, Le-Pape P, Le-Borgne M (2008) Design, synthesis, and evaluation of 1-(N-benzylamino)-2-phenyl-3-(1H-1,2,4-triazol-1-yl)propan-2-ols as antifungal agents. Bioorg Med Chem Lett 18:1820–1824

Goulart DS (2011) Detecção de resíduos de soluçõessanitizantesempregadasempedilúvio para bovinos no leite e solo, MestradoemCiência Animal, Escola de Veterinária e Zootecnia da Universidade Federal de Goiás. p.65.

Ibrahim MM, Mersal GAM, Al-Juaid S, El-Shazly SA (2014) Syntheses, characterization, and SOD activity studies of barbital-based nickel(II) complexes with different chelating amines: The X-ray crystal structures of Barb-H and [Ni(Barb)2(en)2] (Barb = 5,5-diethylbarbiturate). J Mol Struct 1056–1057:166–175

Kathiravan MK, Salake AB, Chothe AS, Dudhe PB, Watode RP, Mukta MS, Gadhwe S (2012) The biology and chemistry of antifungal agents: a review. Bioorg Med Chem 20:5678–5698

Khan A, Ahmad A, Manzoor N, Khan LA (2010) Antifungal activities of *Ocimum sanctum* essential oil and its lead molecules. Nat Prod Commun 5:345–349

Lever ABP (1968) The electronic spectra of tetragonal metal complexes: analysis and significance. Coord Chem Rev 3: 118–140

Liu F, Luo XQ, Song BA, Bhadury PS, Yang S, Jin LH, Xue W, Hu DY (2008) Synthesis and antifungal activity of novel sulfoxide derivatives containing trimethoxyphenyl substituted 1,3,4-thiadiazole and 1,3,4-oxadiazole moiety. Bioorg Med Chem 16:3632–3640

Nandy M, Shit S, Rizzoli C, Pilet G, Mitra S (2015) Syntheses, characterization, and crystal structures of few dioxomolybdenum (VI) complexes incorporating tridentate hydrazones. Polyhedron 88:63–72

Naskar S, Mishra D, Chattopadhyay SK, Corbella M, Blake AJ (2005) Versatility of 2,6-diacetylpyridine (dap) hydrazones in stabilizing uncommon coordination geometries of Mn(II): Synthesis, spectroscopic magnetic and structural characterization. Dalton Trans 2428-2435.

Özer CK, Arslan H, Van Derveer D, Külcü N (2009) Synthesis and characterization of N-(arylcarbamothioyl)-cyclohexanecarboxamide derivatives: the crystal structure of N-Naphthalen-1-ylcarbamothioyl)cyclohexanecarboxamide. Molecules 14:655–666

Poulain D (2013) Candida albicans, plasticitéetpathogénie. . Rev Francophone Lab 2013:37–46

Rakha TH, El-Gammal OA, Metwally HM, Abu El-Reash GM (2014) Synthesis, characterization, DFT and biological studies of (Z)-N ′-(2-oxoindolin-3-ylidene)picolinohydrazide and its Co(II), Ni(II) and Cu(II) complexes. J MolStruct 1062:96–109

Rollas S, Kucukguzel SG (2007) Biological activities of hydrazone derivatives. Molecules 12:1910–1939

Sadek B (2011) Imidazole-substituted drugs and tendency for inhibition of cytochrome P450 isoenzymes: a review. Der Pharma Chemica 3:410–419

Singh DP, Kumar R, Malik V, Tyagi P (2007) Synthesis and characterization of complexes of Co(II), Ni(II), Cu(II), Zn(II), and Cd (II) with macrocycle 3,4,11,12-tetraoxo-1,2,5,6,9,10,13,14-octaaza-cyclohexadeca-6,8,14,16-tetraene and their biological screening. Trans Metal Chem 32:1051–1055

Stadler A, Harrowfield J. (2009) Bis-acyl-/aroyl-hydrazones as multidentate ligands. J Inorg Chim Acta 362:4298–4314

Subramanya GS, Dharavath S, Satyanarayan P, Samudranil P (2003) Co(II) and Co(III) complexes with N-(aroyl)-N'-(picolinylidine) hydrazines. Spin cross over in Co(II) complexes. Ind J Chem 42A:2352–2358

Vandeputte P, Ferrari S, Coste AT (2012) Antifungal resistance and new strategies to control fungal infections. Int J Microbiol 2012:713687

Wani MY, Bhat AR, Azam A, Athar F (2013) Nitroimidazolylhydrazones are better amoebicides than their cyclized 1,3,4-oxadiazoline analogues: In vitro studies and lipophilic efficiency analysis. Eur J Med Chem 64:190–199

Wani MY, Bhat AR, Azam A, Choi I, Athar F (2012) Probing the antiamoebic and cytotoxicity potency of novel tetrazole and triazine derivatives. Eur J Med Chem 48:313–320

Wani MY, Bhat AR, Azam A, Lee DH, Choi I, Athar F (2012) Synthesis and in vitro evaluation of novel tetrazole embedded 1,3,5-trisubstituted pyrazoline derivatives as Entamoeba histolytica growth inhibitors. Eur J Med Chem 54:845–854

Yan-Hui S, Jie L, Jia L, Xue-Zhi S (2007) Synthesis, crystal structures and properties of two novel macrocyclic nickel(II) and copper(II) complexes. J MolStruct 837:257–262

Zhang L, Peng XM, Damu GL, Geng RX, Zhou CH (2014) Comprehensive review in current developments of imidazole-based medicinal chemistry. Med Res Rev 34:340–437